Journal of Applied Mechanics and Technical Physics, Vol. 42, No. 1, pp. 174–184, 2001

CONTAINER FOR LOCALIZATION OF AN EXPLOSION OF A COMPACT HIGH-EXPLOSIVE CHARGE WITH AN INERT SHELL

A. G. Ivanov, M. A. Syrunin, and A. G. Fedorenko

UDC 624.074.4:678.067

Results of an experimental study of fragmentation effects in the explosion and the piercing power of the fragments of inert masses in the form of hemispherical aluminum and soft-steel shells enclosing the spherical charge of a high explosive under their action on flat steel, aluminum, steel-net, and claydite–concrete barriers are given. A design of the lightest spherical explosion-proof container with a load-carrying steel or glass-reinforced plastic shell protected by a splinter-proof layer capable of withstanding an explosion of a high-explosive charge (with a twofold safety factor) with an inert steel shell is proposed.

The possibility of using two-layer spherical glass-reinforced plastic and steel shells as a carrying case of lightest-weight containers localizing an explosion of a high-explosive (HE) charge is shown in [1–4]. Shells of this type are a factor of 5–10 lighter than similar shells from structural steels. They have great specific explosion safety (the ratio of the HE mass to the mass of the case reaches 1/20–1/17), the load-carrying glass-reinforced plastic layers are not sensitive to the scale effects of energetic nature and have a number of other advantages compared to structures made from homogeneous materials [3]. However, the use of such load-carrying shells in protective containers is limited because of the fact that the load-carrying layer can be damaged under the action of high-speed fragmentation-type elements. For example, in the explosion of an HE charge with an inert case in the ammunition or in a terrorist explosive system, the case shell is fragmented, and the fragments (splinters) have quite a high speed and significant piercing power. Thus, alongside with the demolition effect of the shock wave and the gaseous explosion products, a protective container intended to ensure the safety of an explosion-hazardous object (for example, upon storage and transportation) should sustain impacts of high-speed splinters. In some cases, it is necessary to preserve not only the structural integrity of the container but also its tightness. Therefore, in addition to an airtight load-carrying shell, the container should have a protective splinter-proof layer [2, 5].

The main goal of this work is to study experimentally the strength and dynamic reaction of a spherical glass-reinforced plastic container reinforced by a steel layer (see [2–4, 6]) with the splinter-proof protection selected in model experiments in the case where an HE charge with an inert shell explodes in the container.

1. Explosive Fracture of Thin-Walled Metal Shells and Their Effect on Barriers. As an inert outer shell enclosing a spherical HE charge, the constant-thickness hemispherical shells made from steel or aluminum alloy, adjacent to the HE surface, and butted together without fixing the sides were used. The mass of these shells was about 0.3 of the HE mass. In this case, in the explosion, the shell adjoining to the HE takes off the maximum amount of energy, which can be estimated from the data in [7].

Under explosive loading of the shells, the cast spherical HE charges made from a 50/50 TNT/RDX alloy were used; their mass differed by approximately a factor of 20.

Russian Federal Nuclear Center, Institute of Experimental Physics, Sarov 607190. Translated from Prikladnaya Mekhanika i Tekhnicheskaya Fizika, Vol. 42, No. 1, pp. 196–208, January–February, 2001. Original article submitted September 1, 1999; revision submitted May 10, 2000.

TABLE 1

M_{HE}, kg	R_{HE}, mm	Δ, mm		M_{i}, kg		L, mm	
		steel	aluminum	steel	aluminum	steel	aluminum
5.17	90	2.11	5.84	1.666	1.771	400 ± 15	400 ± 30
0.935	51	1.33	3.43	0.3085	0.3085	250 ± 30	250 ± 30
0.248	33	0.77	2.12	0.0564	0.0725	148	148

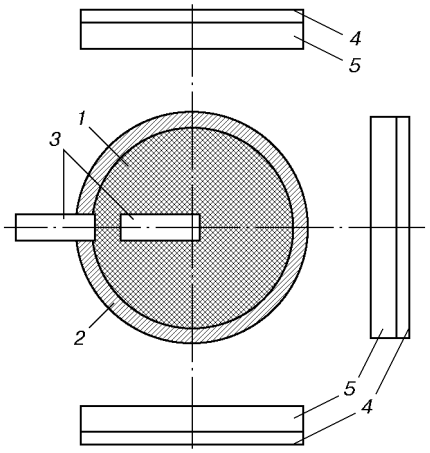

Fig. 1. Experimental scheme: 1) HE charge; 2) inert shell; 3) electric detonator (placed on the surface or at the center of the HE charge depending on experimental conditions); 4) steel sheet of thickness 2–3 mm; 5) barrier.

Table 1 gives values of the radius (R_{HE}) and mass (M_{HE}) of HE charges, the thickness Δ, the distance from the center of the charge to the barrier L, and the masses of inert shells M_{i} made from steel ($\rho_0 = 7800$ kg/m^3) and aluminum ($\rho_0 = 2700$ kg/m^3). The HE charge was initiated by an electric detonator at a point on the surface or at the center.

To determine the number of splinters and their affection and to study the protective properties of some materials, the barriers (screens) were placed at distances $L \approx (4.4\text{–}4.9)R_{\mathrm{HE}}$ from the center of the charge. The distance L was selected depending on the distance from the center of an HE to the wall of the explosion-proof container for the cavity diameter ranging from 300 to 800 mm; this is necessary to assess the influence of the change in the scale on the parameters that characterize the action of splinters. The barriers were shaped like flat plates of thickness h and dimension 0.5×0.5 m and they were made from soft steel, aluminum alloy, claydite–concrete, or a metal net with 2-mm cells and wire diameter 0.5 mm [5, 8]. In preliminary experiments, under the action of compact masses imitating a high-speed splinter (a steel sphere of diameter 14 mm and mass 12 g accelerated to the velocities 0.8 and 1.6 km/sec was used as a compact mass); we note that the indicated materials had quite good protective properties [8]. Behind each barrier (except for steel barriers), a steel sheet of thickness 2–3 mm imitating the wall to be protected was placed immediately adjacent to the barrier. The experimental scheme is depicted in Fig. 1. Tests with $M_{\mathrm{HE}} = 0.248$ kg were carried out in cylindrical tubes (the inner diameter was 296 mm and the length was 600 mm) with an internal steel layer of thickness 2 mm and the outer glass-reinforced plastic layer of thickness 9 mm. The screens of other types were not used. The main experimental results concerning explosive fracture of spherical shells from within with the use of barriers made from different materials are listed in Tables 2 and 3.

In tests, the velocity of splinters V, the number of damages on the barrier surface n, the maximum depth h_1 of craters formed under the action of splinters (Table 2), and the state of the barrier and the protected wall (Table 3) were determined. Figure 2 shows photographs of the barriers made from aluminum alloy and steel after splitting.

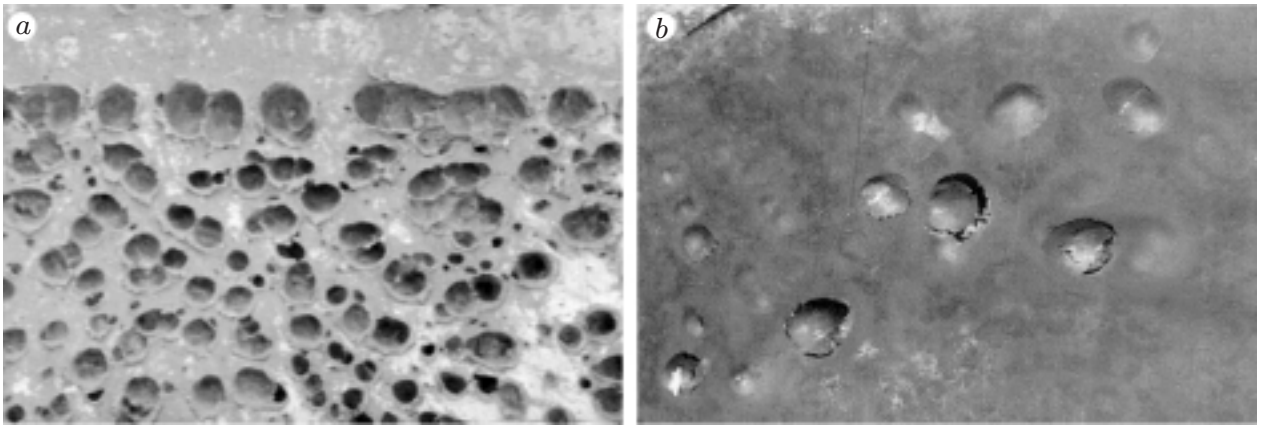

Fig. 2. Barriers made from aluminum alloy from the side of the explosion (a) and soft-steel barriers from the rear side (b) after loading in test No. 1 (Table 4).

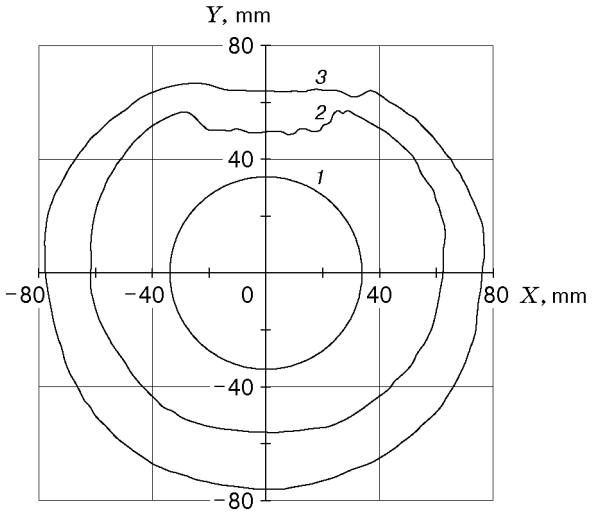

Fig. 3. Scatter of a spherical shell made from St. 3 steel ($R_0 = 33.8$ mm) for $t = 0$ (1), 17.05 (2), and 21.6 μsec (3).

In tests with HE charges ($M_{\text{HE}} = 0.248$ and 0.935 kg) having steel or aluminum-alloy shells, x-ray one-frame streak recording [9] was performed at different moments of time before and after fragmentation of the shells. As a rule, the streak records were obtained in two similar experiments at different moments after initiation of the HE charge. The result of processing of x-ray streak records on the scatter of the St. 3 steel shell with the outer radius of the surface $R_0 = R_{\text{HE}} + \Delta$ ($R_{\text{HE}} = 33$ mm and $M_{\text{HE}} = 0.248$ kg) is shown in Fig. 3 (t is the time from the moment of supply of the initiating pulse at the detonator to the moment of recording).

In tests with HE charges ($M_{\text{HE}} = 5.17$ kg), the extension of the shell after an explosion of an HE charge was registered by a high-speed streak camera in a "time magnifier" mode [10]. The streak recording of fracture of a steel shell is given in Fig. 4.

The average values of the velocities (V) of the splinters of the steel and aluminum shells were 2.7–3.0 km/sec (see Table 2); as in [7], they are almost the same for the shells made from different materials. The shell reaches the maximum velocity at the initial stage of motion for a few microseconds, and then the velocities of the shell and the splinters formed from it increase insignificantly.

In initiating the HE charge at the center and at the surface, the scatter was not radially symmetric owing to the specific features of initiation and unloading on the junction line of hemispherical shells. In processing the results, the average radial velocity of shell scatter was calculated. Estimates that were made

TABLE 2

Test number	M_{HE}, kg	Shell material	V, km/sec	Steel net		Aluminum		Claydite-concrete		Steel		n,
				h, mm	h_1, mm	h, mm	h_1, mm	h, mm	h_1, mm	h, mm	h_1, mm	
1	5.17	Steel	2.89	35–50 (40 layers)	<50 (<40 layers)	20	⩾20	60, 80	⩽60	10	⩾10	4970
2	5.17	Aluminum	2.84	35–50 (25 layers)	<50 (<40 layers)	20	20–26*	50, 70	⩽50	10	8.5	4500
3	0.935	Steel	3.0**	20–40 (25 layers)	<40 (∼20 layers)	15	12	30, 50	30–50	8	5	3804
4	0.935	Aluminum	2.73	20–35 (25 layers)	<35 (<20 layers)	12	⩾12	30, 50	⩽30	10	4	3070
5	0.248	Steel	3.01	—	—	—	—	—	—	2	⩾2	3350
6	0.248	Aluminum	2.87	—	—	—	—	—	—	2	⩾2	2800

Notes. The values of h_1 in experiments with claydite-concrete and in some tests with a steel net cannot be determined because of fracture of the barrier. One asterisk means that the depth of crater is larger than the thickness owing to the formation of a bulge on the rear side; two asterisks refer to the calculated value.

TABLE 3

Test number (see Table 2)	Steel net		Aluminum		Claydite–concrete		Steel	
	State of the barrier	State of the wall behind the barrier	State of the barrier	State of the wall behind the barrier	State of the barrier	State of the wall behind the barrier	State of the barrier	State of the wall behind the barrier
1	Through punctures in some of the layers	No damage	Craters; no through punctures	Hollows	Fractured	No damage	Craters; spalling fracture	No wall
2	The same	The same	The same	The same	The same	The same	Craters; no through punctures	The same
3	〃	〃	Craters; no through punctures, spalling fracture	〃	〃	Through punctures behind a layer 30 mm thick	The same	〃
4	〃	〃	Craters; not through punctures	〃	〃	No damage	〃	〃
5	—	—	—	—	—	—	Through punctures	No through punctures on the glass-reinforced plastic wall
6	—	—	—	—	—	—	The same	The same

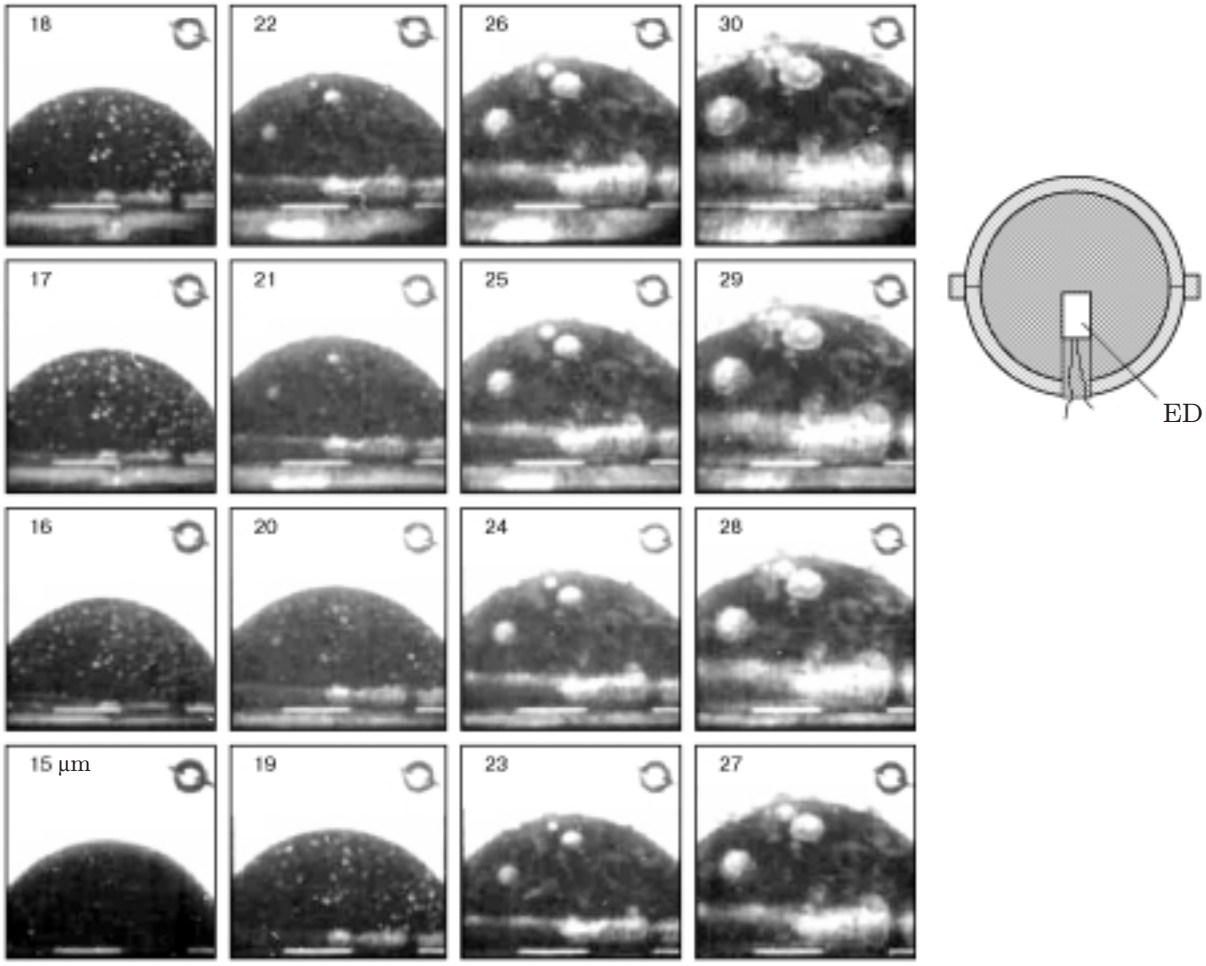

Fig. 4. Streak recording of the scatter and fracture of the steel shell with change of frames for 1 μsec; ED is an electric detonator, the HE charge was initiated at the center, $R_{\text{HE}} = 90$ mm, $\Delta = 2.11$ mm, test No. 1 (Table 2).

with allowance for the average-velocity estimates obtained show that the kinetic energy of the extending shell is 21.5–28.9% of the total energy released in the explosion of the HE charge.

The number of splinters n formed in the explosion was estimated with the use of the product of the number of craters on the barriers N_{b} by the coefficient $4\pi R^2/S_{\text{b}}$ (R is the distance from the HE center to the barrier and S_{b} is the area of the central projection of the barrier upon a sphere of radius R) (see Table 2). In experiments in which a tube served as a barrier (see Table 2, test Nos. 5 and 6), the number of splinters was estimated on the basis of the number of craters on the central annular band of a steel tube of width 50 mm with conversion to the complete stereoscopic angle. A detailed analysis of the results of these experiments is given in [11]; here we present only the basic data used to estimate the splinter-proof parameters.

The following specific features of fracture of spherical shells under internal explosive loading have been revealed:

— formation of the concentric annular lines of splinters (see Fig. 2a);

— insignificant change in the velocity and number of splinters depending on the azimuth angle (see Figs. 2a and 3);

— different dimensions of splinters and the dependence of the piercing power on these dimensions (the depth of craters).

In initiating the HE charge at the center or at the surface, the number of formed splinters (within the limits of estimation error) and their piercing power are approximately the same.

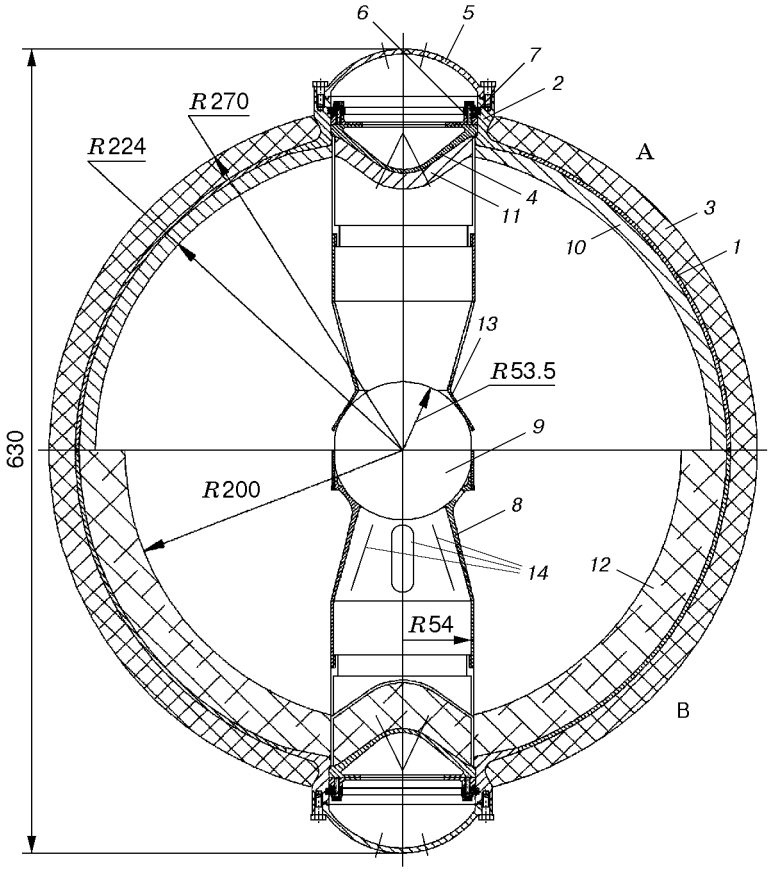

Fig. 5. Design of an explosion-proof container with an aluminum protective splinter-proof layer of thickness 12 mm (A) and with a claydite–concrete layer of thickness 40 mm (B): 1) steel shell; 2) throat; 3) glass-reinforced plastic shell; 4) cover; 5) protecting cap; 6) fixing ring; 7) lock ring; 8) hardened support; 9) spherical HE charge with a shell consisting of steel hemispheres; 10–12) protective splinter-proof layers; 13) nonhardened support; 14) holes in the cones to decrease the explosive load on the covers and throats.

It follows from the experiments that if the values of the masses of inert shells and the initial velocity of scatter are close, the splinters of the soft-steel shell possess a greater piercing power compared to the splinters of the aluminum shell (see Table 2).

In addition, on the screens from a homogeneous material, alongside with the craters formed under the action of splinters (see Fig. 2a), spall bulgings with partial or complete separation of the layer of the material whose thickness is approximately 1–2 mm (see Fig. 2b) form on the rear side opposite some craters. Despite damage or complete fracture, all the materials used as protective splinter-proof layers allow one to damp most of the kinetic energy of the splinters owing to the selected thickness and ensure the intactness of the layer to be protected.

It follows from Table 2 that as the scale of the setup is increased by a factor of 2.7, the number of splinters of the steel and aluminum shells increases by a factor of 1.5–1.6; this shows the presence of scale effects upon explosive fragmentation, which were noted in [12]. The decrease in the relative size of fragments as the scale is increased is likely to be due to the dependences of the specific energy of fracture on the scale and the dynamic yield point on the strain rate.

2. Results of Explosive Tests of the Container. The explosion-proof container to be tested is shown schematically in Fig. 5. The containers consisting of a load-carrying shell similar to that tested in the experiments described in [4] and a splinter-proof layer were tested. The load-carrying shell had an internal soft-steel layer (St. 20 steel of thickness 3 mm and outside diameter of 500 mm) on which an oriented-glass-

TABLE 4

Test No.	ρ, kg/m^3	$2R_{\text{out}}$, mm	M_{case}, kg	M, kg	M_{i}, kg	M_{HE}, kg	$\dot{\varepsilon}_m$, sec^{-1}	ε_y, %	t_y, μsec	ε_x, %	t_x, μsec	ε_{th}, %	t_{th}, μsec	T, °C	t_T, sec
1	2700	526	47.6	76.5	0.227	0.935	320	2.6	260	0.9	160	0.4	235	220	∼100
2	815	532	48.2	72.5	0.406	0.933	255	2.5	310	1.3	275	0.85	245	—	—
3	1160	535	47.1	78.0	0.287	0.944	275	2.2	300	1.5	310	1.2	245	55	∼1600

Notes. In test No. 1, the shell with the first type of reinforcement and the support A (see Fig. 5) were used; in test No. 2, the shell with the second type of reinforcement and the support B (see Fig. 5) were used; in test No. 3, the shell with the second type of reinforcement and a support in the form of a metal pin were used, the protective layer was made from claydite–concrete.

reinforced plastic layer of thickness 14–24 mm on the basis of magnesium–aluminosilicate glass-reinforced plastic (the diameter of an elementary filament is 0.01 mm, the density $\rho = 2490$ kg/m^3, the fracture stress $\sigma_{\text{fr}} = 4.4$ GPa, the limiting deformation is 4.6–5.4%, and Young's modulus $E = 94.75$ GPa) was wound from the outside. The wound layer consisted of several bands from RVMPN 10-1200-78 bundles impregnated with an ÉDT-10 epoxy resin. As in [4], the glass-reinforced plastic layers with two types of reinforcement were tested: 1) with gradual increase in the glass-reinforced plastic thickness from the equator to the throat; 2) with an almost constant thickness [6]. The splinter-proof layer was placed over the entire internal surface of the load-carrying shell and on the protecting caps of the throats. On the basis of the results of the experiments described above and with allowance for the production processes and cost, as a splinter-proof protection for containers, an aluminum alloy Al-9 (variant A in Fig. 5) and a cement solution-set claydite–concrete (variant B) were used. In the repeated test, the density of claydite–concrete was increased.

The diameter of the holes in the throats was 109 mm (0.218 of the diameter of the basic steel shell). The hatches of the throats were closed by high-strength covers [13] supporting on a cut ring fixed by a lock ring. The object was loaded by an explosion of a spherical high-explosive charge enclosed by a steel shell and located at the center of the container hollow. The HE was initiated on the surface of a sphere in test Nos. 1 and 2 and at the center of the sphere in test No. 3. Three variants of the support of the HE charge were used: two variants of conic supports made from aluminum alloy (whose structure is shown in Fig. 5) and a metal pin with a charge on it fixed by a fabric cover. The hollow of the model was filled with air at atmospheric pressure.

In the experiments, the strains of the shell and the throats in time $\varepsilon(t)$ were recorded by the high-speed photorecording and strain-measurement method; the heating of the steel layer of the case was recorded as was done in [4]. The values of the parameters of the tested containers (the density of the protective splinter-proof layer ρ, the mass of the case without sprinter-proof protection M_{case}, the total mass of the case M, and the outer diameter of the case $2R_{\text{out}}$) and the HE charge (50/50 TNT–RDX alloy) in an inert medium (the charge mass M_{HE} and the mass of steel hemispheres M_{i}) and the main experimental results are given in Table 4. In this table, the values of the following parameters averaged over 2–4 measurements are given on the basis of measurement results with an error not greater than 10%: the maximum circumferential (ε_y) and meridional (ε_x) strains reached in the central equatorial cross section of the glass-reinforced plastic shell, the maximum strain of the throat ε_{th}, and the maximum increase in the temperature T on the outer surface of the steel layer of the case and corresponding times t_y, t_x, t_{th}, and t_T from the moment of HE initiation before reaching the maximum strains and temperature. The maximum strain rate was calculated from the formula $\dot{\varepsilon}_m = \max\left(d\varepsilon_y(t)/dt\right)$. Oscillograms of the circumferential strain at the equator are shown in Fig. 6. This figure also shows oscillograms obtained in experiments with spherical containers in the explosion of an HE charge without an inert medium ($M_{\text{HE}} = 1.4$ kg of TNT) [4].

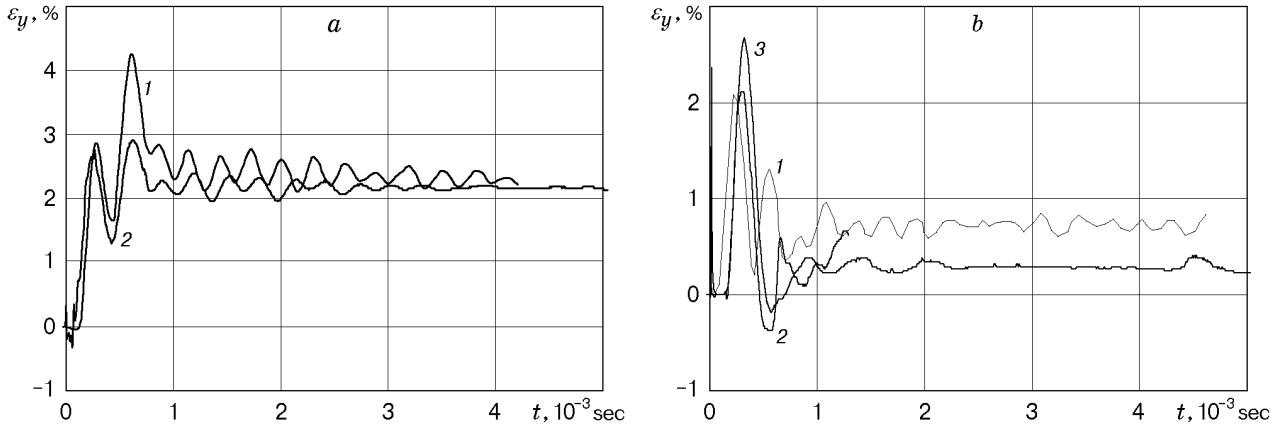

Fig. 6. Oscillograms of the dynamic circumferential strains of the case at the equator for the first (a) and second (b) types of reinforcement: (a) curves 1 and 2 refer to the data from [4] and test No. 1 (Table 4), respectively; (b) curves 1 refer to the data from [4] and curves 2 and 3 refer to the data from test Nos. 3 and 4 (Table 4), respectively.

The experimental results have shown the following. As in the experiments with the HE without an inert medium, in the performed experiments, for the explosive power of an HE whose mass is 1.0–1.4 kg of TNT, the load-carrying case preserves its structural integrity. The changes in its diameter and length are insignificant [in test No. 1 (Table 4), the residual increases in the diameter and length were 1.2% and 0.26%, respectively, in test No. 2, the diameter increased by 0.11%, and in test No. 3, and the diameter and the length increased by 0.24% and 0.78%, respectively]. Only in test No. 2 (Table 4), was one of the throats separated, and the load-carrying (glass-reinforced plastic) layer was damaged in the separation zone. Separation of the throat, apparently, occurred because of the local increase in the load (focusing) owing to the specific design used in this test (the heavier and more rigid support of the charge, and the inert-medium mass was increased by a factor 1.4). In particular, in contrast to test No. 2, in test No. 3 in which the HE was supported by a pin and the inert mass was decreased from 0.406 kg to 0.287 kg, fracture (separation of the throat) did not occur (Table 4). We note that in test No. 2 (Table 4), the supports, which were intended to eliminate the increase in loading on the throats in using a rigid and high-strength support for the HE, had no holes (see Fig. 5). The possibility of local increase in gas-dynamic loading on the cover in a high-strength support (see variant B in Fig. 5) was confirmed by calculations and model experiments.

The maximum dynamic strains of the case were smaller in the shell with the second type of reinforcement; they were reached at the equator and did not exceed 2.2–2.5% (Table 4), which is 27–35% smaller than the minimum limiting dynamic strains (3.4%) for similar cylindrical shells [3, 14].

In [14, 15], it was found in experiments with cylindrical shells, that the limiting strain of dynamic expansion of oriented glass-reinforced plastices depends weakly on the scale effect, the reinforcement structure (in the presence of layers with filaments located in the direction of expansion), and the degree of biaxiality of the stress state with a characteristic strain rate of 10^2–10^3 $\sec^{-1}$. These conclusions are supported in the experiments reported in [4], in which the maximum strains up to 4.9% were reached in spherical shells with the first type of glass-reinforced plastic reinforcement without fracture. If the limiting strain of a second-type shell is also not smaller than 4.9%, we obtain a safety factor not smaller than 1.9–2.3.

The dynamic response of the case in the presence of a splinter-proof layer is similar to the response of the case without this layer. However, in the case of a claydite–concrete splinter-proof layer, the excited oscillations have a lower frequency and damp more rapidly (for 1–2 msec) (see Fig. 6). The established level of strains for both types of protective layer and shell reinforcement is, as a rule, lower than in the tests with a splinter-free explosion, which ensures higher strength for the quasistatic phase of residual-pressure loading.

The maximum circumferential strains of the throats are smaller than on the case and are not greater than 1.0–1.5% (this is confirmed by the data from [4]), and the residual strain is not greater than 0.7%. Such

strains cannot infringe the coupling of the cut supporting rings holding the hatch covers, with a groove in the throat. At the same time, in test No. 2 (Table 4), separation of the throat did not exert an effect on its deformation upon dynamic extension. The simultaneous fracture of the covers, the supporting (cut) rings, and the weld seam of fixing of the throat to the case, which was observed in this test, shows the almost identical strength of these elements. In [13], a similar high-strength cover was loaded by an explosion of a 2.6-kg sphere of an HE consisting of TNT–RDX alloy in an open hemispherical hollow with a 500 mm diameter equal to the diameter of the container shell. Here the residual strain in the cover was smaller than 1%, which shows the reliability of the airtight units of the container.

It follows from the temperature measurement results that to decrease the thermal loads on the load-carrying layer, a claydite–concrete protection with the use of which the heating of the steel layer does not exceed 55–80°C is preferred. This temperature is a factor of 2 lower than the temperature upon thermal treatment of glass-reinforced plastic, which is necessary for polymerization of the epoxy resin of the binder and, consequently, does not lead to its fracture. It is noteworthy that the maximum quasistatic pressure of the explosion products because of the heat transfer to the wall decreases rapidly, and a pressure much smaller than at the beginning acts on the heated load-carrying glass-reinforced plastic layer.

An analysis of the results of test No. 1 (Table 4) shows that the heating of the steel layer of the case up to 220°C could be caused by additional energy release owing to alumothermal reactions of the explosion-sprayed aluminum contained in the support units and the splinter-proof protective layer with oxygen. However, this explanation of the heating of the case to the indicated temperature calls for a more detail study and goes beyond the scope of this paper. Nevertheless, this variant of protection of the case in the test ensured its carrying power and airtightness [even when the first (weaker) type of winding of the composite layer was used].

The results of experiments with flat steel and aluminum barriers also show that under the action of splinters, spalls appeared in these barriers. According to the data from [12], glass-reinforced plastic has insignificant spalling strength in the direction normal to the surface of the container shells, and splinter-generated shock waves propagate in this direction to the wall. Therefore, spalling can occur in glass-reinforced plastic. However, in experiments with a container with a protective layer made from aluminum alloy contacting with a two-layer case, no apparent damage of the outside composite layer was observed. Therefore, since the strength of the metal layer is greater compared to the claydite–concrete layer for close masses, one can use it in an explosion-proof container as a load-carrying and hermetic layer and a splinter-proof protective layer.

In test No. 3 (Table 4), in which there was no aluminum inside the hollow, under a loading close to the limiting explosive central-symmetric loading, the predicted dynamic and quasistatic strengths and the tightness of the explosion-proof container were confirmed.

3. Conclusions. Thus, the experimental data on fragmentation and subsequent scatter of the splinters of an inert thin-walled spherical shell made from soft steel or aluminum alloy in the explosion of spherical HE charges allow one to estimate some parameters of the formed splinters. The average velocities of the fragments of the steel and aluminum shells were 2.7–3.0 km/sec, and the splinters were 2800–5000 in number depending on the dimension and material of the shell. Some specific features of fragmentation of soft-steel and aluminum shells have been revealed. However, to determine the sizes and masses of splinters, it is necessary to perform experiments with catching without additional fracture of all the splinters.

The experimental results have shown that the high-speed splinters have quite a high piercing power and can lead to spalling damage of a barrier made from a homogeneous material. It has been found that, for close specific masses, the splinters of the steel shell have greater piercing power than those of the aluminum shell.

It has been shown that with increase in the scale of the assembly by a factor of 2.7, the protective barriers made from soft steel, aluminum alloy, claydite–concrete, and a wire fine-cell net of a given thickness allow one to catch almost all the splinters of an inert material formed in the explosion.

On the basis of experimental results, a design of an explosion-proof container which can be used, in particular, for storage and transportation of explosive materials, ammunition, including nuclear weapons [17] and also upon evacuation of damaged ammunition and terrorist explosive systems has been proposed.

The authors are grateful to L. I. Kochkin, A. A. Porfir'ev, and A. P. Tsoi for their assistance in performing the first part of work.

This work was supported by the International Scientific and Technical Center (Grant No. 215-95).

REFERENCES

1. A. G. Ivanov, M. A. Syrunin, and A. G. Fedorenko, "Dynamic strength of spherical shells under internal explosive loading," *Rev. High Pressure Sci. Technol.*, **8**, No. 4, 302–305 (1998).
2. M. A. Syrunin, A. G. Fedorenko, and A. G. Ivanov, "The explosion-proof container, satisfying the IAEA norms on safety," in: *Proc. of the 12th Int. Conf. on the Packaging and Transportation of Radioactive Materials* (Paris, France, May 10–15, 1998), Vol. 4, CFEN, Paris (1998), pp. 1574–1580.
3. A. G. Fedorenko, M. A. Syrunin, and A. G. Ivanov, "Dynamic strengths of shells made from oriented fibrous composites under explosive loading (review)," *Prikl. Mekh. Tekh. Fiz.*, No. 1, 126–133 (1993).
4. A. G. Fedorenko, M. A. Syrunin, and A. G. Ivanov, "Dynamic strength of spherical glass-reinforced plastic shells under internal explosive loading," *Fiz. Goreniya Vzryva*, **31**, No. 4, 93–99 (1995).
5. W. B. Benedick and C. J. Daniel, "Explosion containment device," U.S. Patent No. 4055247 US, F 42 B 37/02; No. 734834, Filed Oct. 22 (1976).
6. A. G. Ivanov, M. A. Syrunin, and A. G. Fedorenko "Method of fabricating a device for localization of explosion products," Russian Patent No. 2009387 RU, S 1 kl. 5 F 17/00, Publ. 03.15.94, Bull. No. 5.
7. A. G. Ivanov, L. I. Kochkin, L. V. Vasil'ev, et al., "Explosive fracture of tubes," *Fiz. Goreniya Vzryva*, No. 1, 127–132 (1974).
8. G. V. Belov, E. P. Dyakin, S. A. Protasov, et al., "Penetration of compact steel projectiles into heterogeneous metal targets of tied-wire fabric (TWF) type," *Int. J. Impact Eng.*, No. 23, 63–66 (1999).
9. J. Gehring, "Hypervelocity impact from the engineering viewpoint," in: *Hypervelocity Impact Phenomena* [Russian translation], Mir, Moscow (1973).
10. A. S. Dubovik, *Photographic Recording of Fast Processes* [in Russian], Nauka, Moscow (1975), pp. 63–68.
11. A. G. Ivanov, M. A. Syrunin, A. G. Fedorenko, and A. P. Tsoi, "Splitting of spherical shells at internal explosive loading," in: *Book of Abstracts of Intern. Conf. on High Pressure Sci. and Technol.* (Honolulu, Hawaii, July 25–30, 1999), Int. Assoc. for the Adv. of High Pressure Sci. and Technol., Honolulu (1999), p. 405.
12. A. G. Ivanov, L. I. Kochkin, V. F. Novikov, and T. M. Folomeeva, "High-speed fracture of thin-walled soft-steel tubes," *Prikl. Mekh. Tekh. Fiz.*, No. 1, 112–117 (1983).
13. A. G. Fedorenko, A. G. Shimarov, and M. A. Syrunin, "Development and test of a high-pressure cap," *Prikl. Mekh. Tekh. Fiz.*, **35**, No. 2, 163–168 (1994).
14. M. A. Syrunin, A. G. Fedorenko, and A. G. Ivanov, "Limiting strain of an oriented glass-reinforced plastic shell under internal explosive loading," *Fiz. Goreniya Vzryva*, **28**, No. 2, 87–93 (1992).
15. A. G. Ivanov, M. A. Syrunin, and A. G. Fedorenko, "Effect of the reinforcement structure on the limiting deformability and strength of oriented-glass-reinforced plastic shells under explosive loading from the within," *Prikl. Mekh. Tekh. Fiz.*, No. 4, 130–135 (1992).
16. A. G. Ivanov, M. A. Syrunin, and A. G. Fedorenko, "Spalling strength of winding glass-reinforced plastic in three main directions," *Probl. Prochn.*, No. 1, 82–88 (1993).
17. A. G. Ivanov, A. G. Fedorenko, and M. A. Syrunin, "Possibility of increasing the safety of nuclear weapons," *Fiz. Goreniya Vzryva*, **31**, No. 2, 169–171 (1995).